



# Inversion and rotation processes involving non-planar aromatic compounds catalyzed by extended polycyclic aromatic hydrocarbons



Amir Karton

School of Chemistry and Biochemistry, The University of Western Australia, Perth, WA 6009, Australia

## ARTICLE INFO

## Article history:

Received 10 August 2014

In final form 11 September 2014

Available online 18 September 2014

Dedicated to Professor Leo Radom on the occasion of his 70th birthday.

## ABSTRACT

Using accurate quantum chemical calculations, we show that extended planar polycyclic aromatic hydrocarbons (PAHs) can efficiently catalyze a range of chemical processes involving non-planar aromatic systems. These include (i) bowl-to-bowl inversion of curved PAHs (e.g. corannulene and sumanene), (ii) 'flip-flop' inversion of helicenes (e.g. benzo[c]phenanthrene), and (iii) rotation about the Ph–Ph bond in biphenyls. Non-covalent  $\pi$ – $\pi$  interactions between the planar catalyst and the substrate stabilize the planar transition structures to a greater extent than they stabilize the non-planar reactants. These result in surprisingly large catalytic enhancements (namely, the reaction barrier heights are reduced by 21–63% of the uncatalyzed reaction barriers).

© 2014 Elsevier B.V. All rights reserved.

## 1. Introduction

Aromatic bowl-shaped hydrocarbons are an important class of strained polycyclic aromatic hydrocarbons (PAHs) in which structural geometry constraints (e.g., a pentagon completely surrounded by hexagons) result in a curved  $\pi$ -system [1–3]. In particular, the smallest bowl-shaped PAHs corannulene and sumanene (**1** and **2**, Figure 1) are fragments of fullerenes and have attracted considerable attention over the past decade due to their unusual reactivity and unique chemical properties [4–16].

Corannulene and sumanene are flexible molecules that exhibit dynamic bowl-to-bowl inversion behavior. For example, bowl-to-bowl inversion in corannulene occurs rapidly at room temperature with an estimated experimental Gibbs free energy barrier of 48.1 kJ mol<sup>−1</sup> [11,12]. Seiders et al. demonstrated that there is a nonlinear relationship between the inversion energy barrier and the depth of the bowl in corannulene derivatives [11]. Accordingly, sumanene, which has a deeper bowl than corannulene, inverts at a slower rate (the experimental activation-energy barrier of deuteriosumanene is 84.9 kJ mol<sup>−1</sup>) [13,14]. Recently, Juriček et al. showed that a synthetic cyclophane receptor can catalyze the bowl-to-bowl inversion of ethyl-substituted corannulene by destabilizing the reactant and stabilizing the transition structure within the highly confined cavity of the cyclophane catalyst [15]. Through dynamic <sup>1</sup>H NMR measurements, they estimated that the catalyst reduces the Gibbs free energy barrier at 190 K ( $\Delta G^\ddagger_{190}$ ) by

~15.1 kJ mol<sup>−1</sup> relative to the barrier of the uncatalyzed reaction [11].

Non-covalent  $\pi$ – $\pi$  interactions play a major role in supramolecular and organic catalysis [17]. The magnitude and importance of these interactions for the chemical reactivity of large molecular systems is only now starting to be realized due to the development of theoretical procedures that can accurately describe London-dispersion interactions and are applicable to large systems [18–20]. In particular, the recent development of dispersion-corrected density functional theory (DFT) and double-hybrid DFT (DHDFT) procedures [21,22]. Here we use these methods to show that extended PAHs such as coronene ( $C_{24}H_{12}$ ) and circumcoronene ( $C_{54}H_{18}$ ) (Figure 2) can catalyze the bowl-to-bowl inversion of curved PAHs such as corannulene and sumanene (**1** and **2**, Figure 1) and that the catalytic enhancements are surprisingly large. In particular,  $\pi$ – $\pi$  interactions between the planar catalyst and the substrate stabilize the planar transition structures to a greater extent than they stabilize the curved reactants and products. The present work goes on to examine 'flip-flop' and rotation processes in other non-planar aromatic systems and shows that the catalytic activity of extended planar PAHs is not limited to bowl-to-bowl inversion processes. We show that coronene can efficiently catalyze the 'flip-flop' inversion of the smallest helicene (benzo[c]phenanthrene) and the rotation about the Ph–Ph bond in biphenyl and substituted biphenyls. The considered catalysts, in particular the larger circumcoronene system, may serve as models for graphene-like structures. Thus, these results suggest that graphene flakes may efficiently catalyze inversion, 'flip-flop', and rotation processes involving non-planar PAHs.

E-mail address: [amir.karton@uwa.edu.au](mailto:amir.karton@uwa.edu.au)

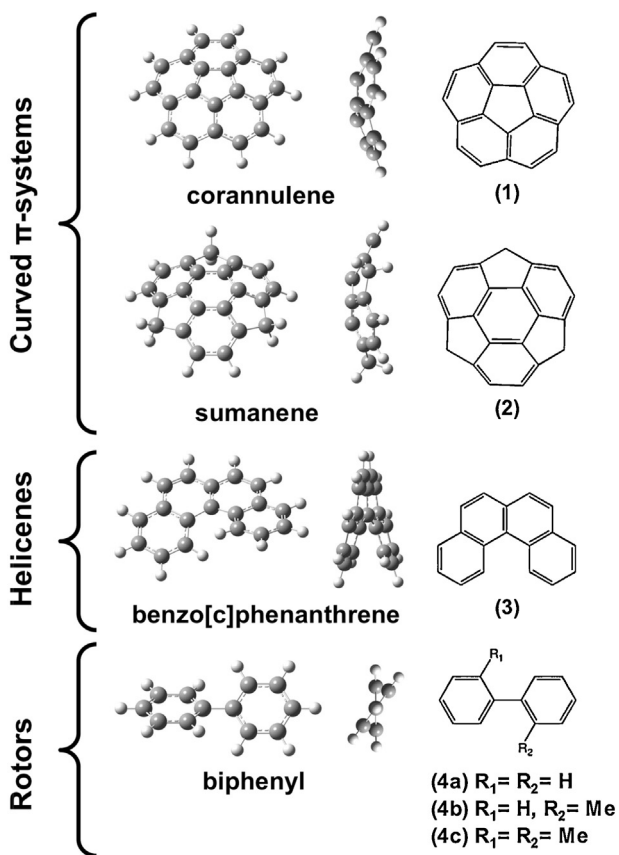


**Figure 1.** Optimized structures of the non-planar aromatic systems considered in this work: front view (left panel), side view (middle panel), and a schematic representation of compounds 1–4 (right panel).

## 2. Computational methods

Double-hybrid DFT calculations [22] were performed in order to obtain accurate energies for the reactant complexes (RC), transition structures (TS), and product complexes (PC) located along the uncatalyzed and catalyzed reaction pathways considered in this work. Two spin-component-scaled DHDFT procedures are employed DSD-PBEP86-D3 [23,24] and PWBP95-D3 [25]. These DHDFT procedures involve both HF-like exchange and MP2-like correlation and have been found to produce thermochemical properties (such as reaction energies and barrier heights) with mean absolute deviations (MADs) approaching the threshold of “chemical

accuracy” (arbitrarily defined as  $1 \text{ kcal mol}^{-1} \approx 4.2 \text{ kJ mol}^{-1}$ ) from a wide range of accurate thermochemical determinations [22–25]. The DHDFT calculations, which inherit the slow basis-set convergence of MP2 to some degree, are carried out with the correlation consistent cc-pVQZ basis set [26]. All DHDFT calculations were performed using the ORCA 3.0.1 program suite [27,28]. The main text reports the DSD-PBEP86-D3/cc-pVQZ results, whereas Table S2 (Supplementary data) compares the DSD-PBEP86-D3/cc-pVQZ and PWBP95-D3/cc-pVQZ reaction barrier heights ( $\Delta G^\ddagger_{298}$ ) for the uncatalyzed and catalyzed reactions. The barrier heights obtained with the two DHDFT functionals agree on average to within  $3.1 \text{ kJ mol}^{-1}$ . For the circumcoronene-catalyzed bowl-to-bowl inversion in corannulene the DHDFT calculations with the cc-pVQZ basis set proved beyond our computational resources. We therefore used the cc-pVTZ basis set in these calculations. Nevertheless, for all the reactions for which we have cc-pVQZ results, the barrier heights obtained with the DSD-PBEP86-D3 functional in conjunction with the cc-pVQZ and cc-pVTZ basis sets agree on average to within  $2.0 \text{ kJ mol}^{-1}$  (Table S2). The geometries of all structures have been obtained at the PBE-D3/6-31G(2df,p) level of theory [29,30]. Empirical D3 dispersion corrections [21,31] are included using the Becke–Johnson [32] damping potential as recommended in Ref. [33] (denoted by the suffix –D3). Gibbs free energies at 298 K ( $\Delta G_{298}$ ) were obtained using the DHDFT electronic energies and the PBE-D3/6-31G(2df,p) zero-point vibrational energies, enthalpic, and entropic corrections. All geometry optimizations and frequency calculations were performed using the GAUSSIAN 09 program suite [34].

For the uncatalyzed reactions involving benzo[c]phenanthrene and biphenyl we were able to perform high-level, ab initio calculations with the W1-F12 thermochemical protocol [35]. All the high-level ab initio calculations were performed using the Molpro 2012.1 program suite [36]. W1-F12 theory represents a layered extrapolation to the relativistic, all-electron CCSD(T) (coupled cluster with singles, doubles, and quasiperturbative triple excitations) basis-set-limit energy, and can achieve “sub-chemical accuracy” for a wide range of thermochemical and kinetic properties (e.g., it is associated with a mean absolute deviation from accurate atomization energies of  $1.3 \text{ kJ mol}^{-1}$ ) for molecules whose wave functions are dominated by dynamical correlation [35,37–41]. We note that for the inversion, rotation, and ‘flip-flop’ processes considered in the present work W1-F12 should yield even better performance due to a large degree of systematic error cancelation between reactants and products. Our DHDFT reaction barrier heights ( $\Delta G^\ddagger_{298}$ ) are in excellent agreement with the barriers obtained from W1-F12 theory, for example, at the DSD-PBEP86-D3/cc-pVQZ level of theory the deviations are smaller than  $1 \text{ kJ mol}^{-1}$  (Table S3, Supplementary data). These small deviations lend confidence to our DHDFT results.

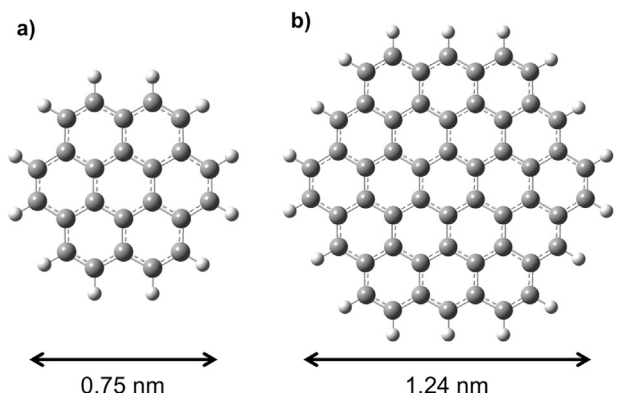


**Figure 2.** Optimized structures of the planar PAH catalysts considered in this work: (a) coronene and (b) circumcoronene. The diameter of the carbon skeleton is given in nm.

## 3. Results and discussion

High-level DHDFT calculations were performed in order to explore the potential energy surface (PES) for the uncatalyzed and catalyzed: (i) bowl-to-bowl inversion in corannulene and sumanene, (ii) ‘flip-flop’ inversion in benzo[c]phenanthrene, and (iii) rotation about the Ph–Ph bond in biphenyl and substituted biphenyls (Figure 1). A common feature shared by these reactions is that the reactants and products have a curved/non-planar  $\pi$ -system whereas the transition structures have a planar  $\pi$ -system (Figure 3).

### 3.1. Catalysis of bowl-to-bowl inversion processes by planar PAHs

Corannulene (**1**, Figure 1) is a flexible bowl-shaped PAH. The depth of the  $C_{5v}$ -symmetric bowl of corannulene, from the plane of

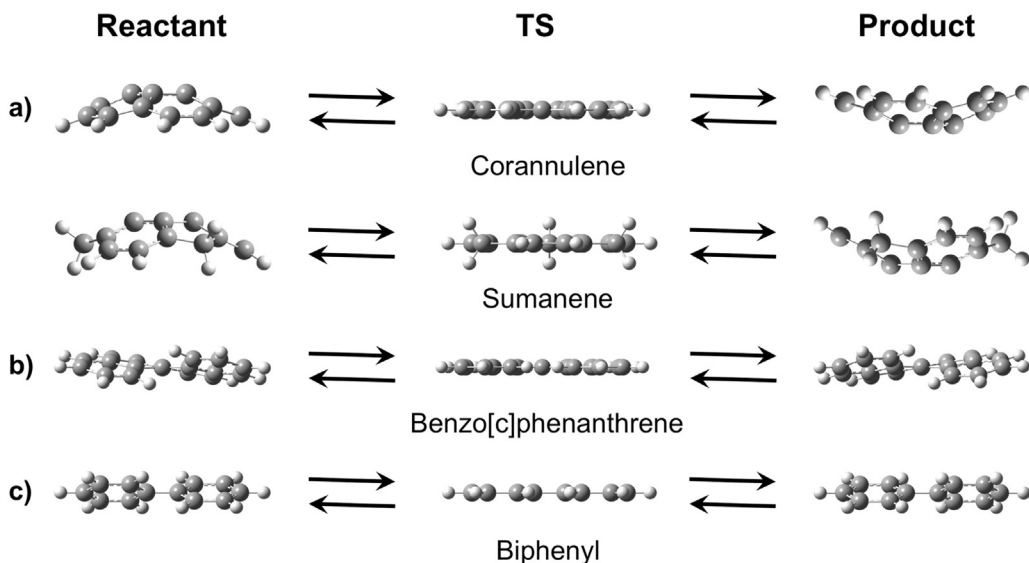


**Figure 3.** Optimized structures for the reactants, transition structures (TS), and products located on the potential energy surface for the uncatalyzed reactions considered in this work: (a) bowl-to-bowl inversion in corannulene and sumanene, (b) 'flip flop' inversion in benzo[c]phenanthrene, and (c) rotation around the single Ph–Ph bond in biphenyl.

the five-membered ring to the plane of rim carbon atoms, is 0.87 Å [42]. The planar conformation of corannulene is a first-order saddle point on the PES connecting the two symmetry-equivalent bowl-shaped local minima (Figure 3). The energy barrier for the bowl-to-bowl inversion has been estimated from dynamic  $^1\text{H}$  NMR measurements of ethyl- and bromomethyl-substituted corannulene

derivatives to be 48.1 kJ mol $^{-1}$  [11]. Table 1 gives the Gibbs free energy barriers at 298 K ( $\Delta G_{298}^\ddagger$ ) for the bowl-to-bowl inversion of corannulene, while the  $\Delta G_{298}$  values for the reactant complexes, transition structures, and product complexes are given in Table S1 (Supplementary data). A schematic representation of the uncatalyzed and catalyzed Gibbs free energy profiles is given in Figure 4.

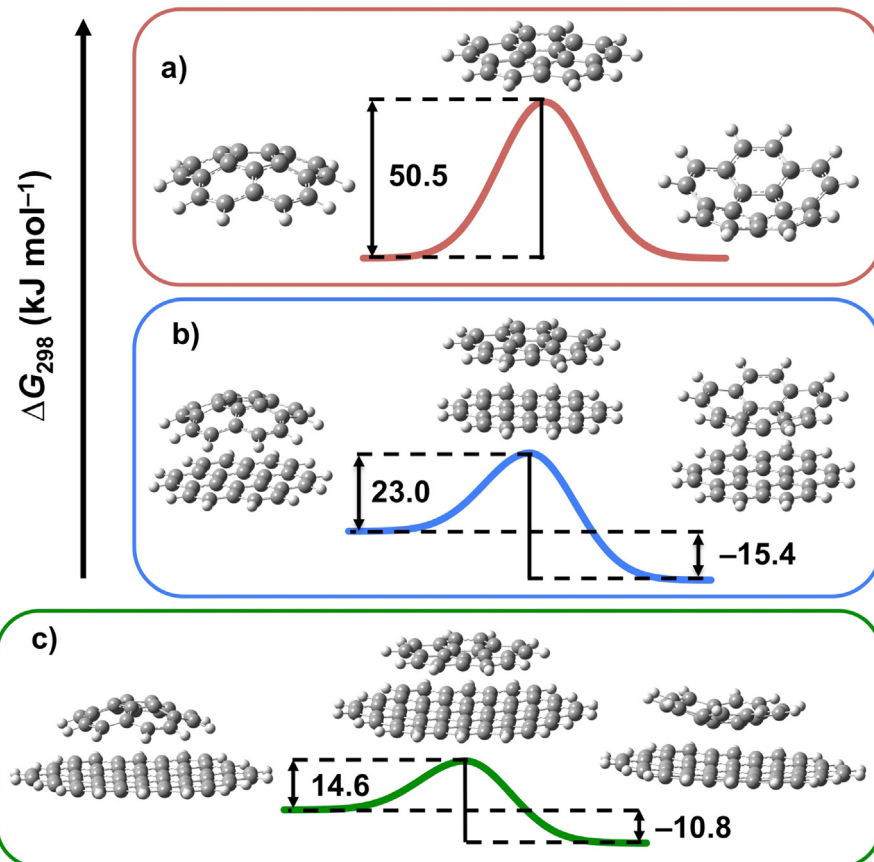


**Figure 4.** Potential energy profiles for the bowl-to-bowl inversion in corannulene: (a) uncatalyzed, (b) catalyzed by coronene, and (c) catalyzed by circumcoronene.

**Table 1**

Gibbs free energies of activation at 298 K ( $\Delta G^\ddagger_{298}$ , DSD-PBEP86-D3/cc-pVQZ, kJ mol<sup>-1</sup>) for the uncatalyzed and catalyzed reactions considered in this work.

System <sup>a</sup>	Catalyst	$\Delta G^\ddagger_{298}$ <sup>b</sup>	$\Delta \Delta G^\ddagger_{298}$ <sup>c</sup>
(1)	Uncatalyzed	50.5	
	Coronene	23.0	27.6
	Circumcoronene <sup>d</sup>	14.6	31.7
(2)	Uncatalyzed	89.4	
	Coronene	66.9	22.5
	Circumcoronene <sup>d</sup>	50.7	35.4
(3)	Uncatalyzed	17.9	
	Coronene	14.3	3.7
(4a)	Uncatalyzed	13.0	
	Coronene	4.8	8.1
(4b)	Uncatalyzed	37.0	
	Coronene	17.0	20.0
(4c)	Uncatalyzed	83.9	
	Coronene	53.4	30.5

<sup>a</sup> Shown in Figure 1.

<sup>b</sup>  $\Delta G^\ddagger_{298}$  values are calculated relative to the RCs.

<sup>c</sup> Catalytic efficiency of the catalyst (see text).

<sup>d</sup> Calculated at the DSD-PBEP86-D3/cc-pVTZ level of theory.

For the uncatalyzed reaction we obtain a barrier of  $\Delta G^\ddagger_{298,\text{uncat}} = 50.5 \text{ kJ mol}^{-1}$ , in good agreement with the estimated experimental value [11]. A coronene catalyst reduces the barrier by more than 50% ( $\Delta G^\ddagger_{298,\text{coronene}} = 23.0 \text{ kJ mol}^{-1}$ ). Taking the catalytic efficiency of the catalyst ( $\Delta \Delta G^\ddagger_{298,\text{cat}}$ ) as the difference in barrier between the uncatalyzed ( $\Delta G^\ddagger_{298,\text{uncat}}$ ) and catalyzed ( $\Delta G^\ddagger_{298,\text{cat}}$ ) reaction barriers (i.e.,  $\Delta \Delta G^\ddagger_{298,\text{cat}} = \Delta G^\ddagger_{298,\text{uncat}} - \Delta G^\ddagger_{298,\text{cat}}$ ), we obtain  $\Delta \Delta G^\ddagger_{298,\text{coronene}} = 27.6 \text{ kJ mol}^{-1}$ . In the RC the concave side of corannulene interacts with the planar catalyst, whereas in the PC the convex side of corannulene faces the catalyst (Figure 4(b)). The attractive  $\pi-\pi$  interactions between corannulene and coronene amount to  $31.3 \text{ kJ mol}^{-1}$  in the RC, and to  $46.7 \text{ kJ mol}^{-1}$  in the PC (Table S1, Supplementary data). We can estimate the transition structure stabilization energy in the catalyzed TS as the energy required to separate the catalyzed TS into the free TS and coronene. This transition structure stabilization energy amounts to  $58.9 \text{ kJ mol}^{-1}$ . Thus, the planar coronene catalyst stabilizes the planar TS to an appreciably greater extent than it stabilizes the curved local minima. The catalytic activity can be attributed to the better overlap between the  $\pi$ -systems of the planar catalyst and substrate in the TS rather than in the RC or the PC.

Table S4 (Supplementary data) compares the bowl depth of free corannulene with that of the RCs and PCs with coronene. The calculated bowl depth decreases along the series: free corannulene > RC with coronene > PC with coronene. Specifically, relative to the bowl depth in free corannulene ( $0.901 \text{ \AA}$ ), the bowl depth decreases by  $0.017$  (RC with coronene) and  $0.084$  (PC with coronene)  $\text{\AA}$ . This trend is consistent with the stronger interaction between corannulene and the catalyst in the PC ( $46.7 \text{ kJ mol}^{-1}$ ) rather than in the RC ( $31.3 \text{ kJ mol}^{-1}$ ) (Table S1, Supplementary data). Thus, stronger  $\pi-\pi$  interaction energies between corannulene and the catalyst lead to a shallower bowl, that is structurally closer to the planar TS, and effectively decrease the energy barrier for the bowl-to-bowl inversion process.

These results are in agreement with experimental and theoretical data that show that corannulene (and related bowl shaped molecules) adopt a shallower bowl upon attractive interactions with metallic surfaces or planar trimeric perfluoro-ortho-phenylene mercury complexes) [43–47].

What about the catalytic activity of larger planar PAHs? Figure 4(c) shows the RC, TS, PC located along the reaction profile for corannulene's bowl-to-bowl inversion catalyzed

by circumcoronene, a 54-carbon-atom graphene nanoflake (Figure 2(b)). Calculating the interaction energies between the circumcoronene catalyst and corannulene in a similar way as described for the coronene catalyst, we obtain interaction energies between circumcoronene and corannulene of  $108.3$  (RC),  $140.0$  (TS), and  $119.1$  (PC) kJ mol<sup>-1</sup> (Table S1, Supplementary data). Thus, similarly to coronene, the circumcoronene catalyst stabilizes the planar TS to an appreciably greater extent than it stabilizes the curved local minima. Overall, a circumcoronene catalyst reduces the reaction barrier height by  $31.7 \text{ kJ mol}^{-1}$  relative to the barrier of the uncatalyzed reaction, and by  $5.1 \text{ kJ mol}^{-1}$  relative to the barrier of the coronene-catalyzed reaction. We also note that the calculated bowl depth of corannulene decreases along the series: free corannulene > RC with circumcoronene > PC with circumcoronene, however, the reduction in the bowl depth in the RC and PC is more pronounced in the corannulene-circumcoronene complexes than in the corannulene-coronene complexes. Specifically, the bowl depth decreases by  $0.030$  (RC with circumcoronene) and  $0.186$  (PC with circumcoronene)  $\text{\AA}$ , relative to the bowl depth in free corannulene (Table S4, Supplementary data). Again, this trend is consistent with the increase in the interaction energies between corannulene and the circumcoronene in the same order: RC with circumcoronene < PC with circumcoronene (Table S1, Supplementary data).

We turn now to the bowl-to-bowl inversion in sumanene (2, Figure 1). For free sumanene we obtain a Gibbs free energy barrier of  $\Delta G^\ddagger_{298,\text{uncat}} = 89.4 \text{ kJ mol}^{-1}$ . This reaction barrier energy is in good agreement with the experimental value obtained by Amaya et al. [5] for trideuteriosumanene from 2D NMR experiments in  $\text{CD}_2\text{Cl}_2$  at  $303 \text{ K}$  ( $\Delta G^\ddagger_{303,\text{uncat}} = 84.9 \text{ kJ mol}^{-1}$ ). A coronene catalyst reduces this barrier by  $22.5 \text{ kJ mol}^{-1}$  ( $\Delta G^\ddagger_{298,\text{coronene}} = 66.9 \text{ kJ mol}^{-1}$ ). Similarly to the bowl-to-bowl inversion in corannulene, this catalytic enhancement originates from the greater stabilization energy provided by the catalyst for the planar TS than to the non-planar local minima. Specifically, the attractive  $\pi-\pi$  interaction energies are  $33.2$  (RC),  $55.7$  (TS), and  $34.6$  (PC) kJ mol<sup>-1</sup> (Table S1, Supplementary data). Similarly to the bowl-to-bowl inversion in corannulene, a circumcoronene catalyst results in a higher catalytic efficiency ( $\Delta \Delta G^\ddagger_{298,\text{coronene}} = 35.4 \text{ kJ mol}^{-1}$ ) compared to that of coronene ( $\Delta \Delta G^\ddagger_{298,\text{coronene}} = 22.5 \text{ kJ mol}^{-1}$ ).

### 3.2. Catalysis of 'flip-flop' and rotation processes by planar PAHs

The results described above show that extended planar PAHs can efficiently catalyze bowl-to-bowl inversion processes in prototypical curved aromatic systems (e.g., corannulene and sumanene). The question that naturally arises is, whether extended PAHs can catalyze other processes involving aromatic systems with a planar TS and non-planar local minima? Here we consider the 'flip-flop' inversion in benzo[c]phenanthrene and the rotation about the Ph–Ph bond in biphenyls.

Benzo[c]phenanthrene is a structural isomer of naphthalene in which the benzene rings are ortho-fused to one another. Benzo[c]phenanthrene adopts a non-planar helical structure (3, Figure 1) that oscillates rapidly between two  $C_2$ -symmetric conformations via a planar TS with  $C_{2v}$  symmetry [48,49]. The calculated dihedral angle between the two terminal rings ( $27.5^\circ$ ) is in good agreement with the experimental value of  $26.7^\circ$  [11]. Our theoretical Gibbs free energy racemization barrier ( $17.9 \text{ kJ mol}^{-1}$ ) is in excellent agreement with the barrier calculated using the high-level ab initio W1-F12 thermochemical protocol ( $\Delta G^\ddagger_{298,\text{uncat}} = 18.8 \text{ kJ mol}^{-1}$ ) [35]. A coronene catalyst reduces this barrier by  $21\%$  ( $\Delta \Delta G^\ddagger_{298,\text{coronene}} = 3.7 \text{ kJ mol}^{-1}$ ). The coronene catalysts stabilizes the non-planar local minima by  $40.2 \text{ kJ mol}^{-1}$  and the planar TS by  $43.9 \text{ kJ mol}^{-1}$  (Table S1, Supplementary data).

As a final example we consider the rotation around the Ph–Ph bond in biphenyl and ortho-substituted biphenyls (**4a–4c**, Figure 1). Biphenyl is a non-planar aromatic compound, in which competition between  $\pi$ -conjugation (which favor a coplanar structure) and steric repulsion of the ortho hydrogens (which favor a non-planar structure) result in a twist angle ( $\theta$ ) between the two Ph rings. The PES for the rotation about  $\theta$  is characterized by two low-lying first-order saddle points at  $\theta=0$  and  $90^\circ$ . Here we are interested in the planar TS (at  $\theta=0^\circ$ ). Our theoretical rotational barrier ( $\Delta G^\ddagger_{298,\text{uncat}} = 13.0 \text{ kJ mol}^{-1}$ ) is in excellent agreement with the value obtained with the W1–F12 thermochemical protocol ( $\Delta G^\ddagger_{298,\text{uncat}} = 12.2 \text{ kJ mol}^{-1}$ ) [35]. A coronene catalyst reduces this barrier by a significant amount of  $\Delta\Delta G^\ddagger_{298,\text{coronene}} = 8.1 \text{ kJ mol}^{-1}$ . Similarly to corannulene, sumanene, and benzo[c]phenanthrene, the coronene catalyst stabilizes the planar TS ( $30.4 \text{ kJ mol}^{-1}$ ) to a greater extent than it stabilizes the non-planar local minima ( $22.3 \text{ kJ mol}^{-1}$ , Table S1, Supplementary data). We note that the interaction with the coronene catalyst reduces the twist angle in biphenyl by nearly  $13^\circ$  (from  $36.3^\circ$  in free biphenyl to  $23.5^\circ$  in the biphenyl–coronene complex). Thus, the coronene catalyst reduces the rotational barrier by ‘forcing’ biphenyl to adopt a flatter conformation, which in effect decreases the energy barrier for the rotation process. Substitution of one of the ortho hydrogens with a methyl group (2-methylbiphenyl, **4b**, Figure 1) results in a rotational barrier of  $\Delta G^\ddagger_{298,\text{uncat}} = 37.0 \text{ kJ mol}^{-1}$  (Table 1) – an increase of  $24.0 \text{ kJ mol}^{-1}$  relative to the rotational barrier in biphenyl. Similarly to biphenyl, the coronene catalyst stabilizes the planar TS by  $29.0 \text{ kJ mol}^{-1}$ . However, the stabilization provided to the RC ( $9.0 \text{ kJ mol}^{-1}$ ) is smaller than that provided to biphenyl ( $22.3 \text{ kJ mol}^{-1}$ ) (Table S1, Supplementary data). In part, the smaller stabilization may be attributed to the larger twist angle in the 2-methylbiphenyl RC compared to the biphenyl RC (namely,  $44.9^\circ$  and  $23.5^\circ$ , respectively), which reduces the  $\pi$ – $\pi$  overlap between 2-methylbiphenyl and coronene.

What about substitution of an ortho-hydrogen with a methyl group on both rings? The rotational barrier for the uncatalyzed process in 2,2'-dimethylbiphenyl (**4c**, Figure 1) is  $83.9 \text{ kJ mol}^{-1}$  – an increase of  $70.9 \text{ kJ mol}^{-1}$  relative to the rotational barrier in biphenyl. A coronene catalyst reduces this barrier by as much as  $\Delta\Delta G^\ddagger_{298,\text{coronene}} = 30.5 \text{ kJ mol}^{-1}$ . Again, introduction of a second methyl groups has little affect on the stabilization energy provided to the TS (specifically, it amounts to  $29.2 \text{ kJ mol}^{-1}$ ). However, the stabilization provided to the local minima is significantly diminished. Specifically, it is slightly repulsive in the RC ( $\Delta G_{298} = +1.3 \text{ kJ mol}^{-1}$ ) in which both methyl groups are pointing toward the coronene catalyst, and slightly attractive in the PC ( $\Delta G_{298} = -3.5 \text{ kJ mol}^{-1}$ ) in which both methyl groups are pointing away from the planar catalyst. Again, the changes in the stabilization energy provided by the catalyst in the RC and PC may, in part, be attributed to large twist angles ( $67.4$  and  $59.7^\circ$ , respectively).

#### 4. Conclusions

On the basis of high-level computational modeling, we show that extended planar PAHs such as coronene and circumcoronene can efficiently catalyze inversion and rotation processes involving non-planar PAH systems. A common feature shared by these catalyzed processes is that the reactants and products have a curved/non-planar  $\pi$ -system whereas the transition structures have a planar  $\pi$ -system. Non-covalent  $\pi$ – $\pi$  interactions between the planar PAH catalyst and the non-planar aromatic substrate stabilize the TS to a greater extent than they stabilize the local minima. We show that the catalytic enhancements provided by the coronene and circumcoronene catalysts are surprisingly large (namely, they reduce the reaction barrier heights by 21–63% of

the uncatalyzed barriers). Furthermore, this work demonstrates the generality of this catalytic activity. Namely that coronene and circumcoronene can catalyze the following processes: (i) bowl-to-bowl inversion of curved PAHs (corannulene and sumanene), (ii) ‘flip-flop’ inversion of benzo[c]phenanthrene, and (iii) rotation about the Ph–Ph bond in biphenyls. These results suggest that graphene flakes may efficiently catalyze inversion, ‘flip-flop’, and rotation processes involving non-planar PAHs.

#### Acknowledgments

We gratefully acknowledge funding from the Australian Research Council (ARC) (project number: DE140100311) and the generous allocation of computing time from the National Computational Infrastructure (NCI) National Facility, and the support of iVEC through the use of advanced computing resources located at [iVEC@UWA](http://ivec@uwa.edu.au). We would also like to thank the reviewers for helpful comments.

#### Appendix A. Supplementary data

Gibbs free energies ( $\Delta G_{298}$ ) for the species located along the reaction profile for the inversion, flip-flop and rotation processes (Table S1); local minima and transition structures located on the PESs for the bowl-to-bowl inversion of sumanene catalyzed by coronene and circumcoronene (Figure S1); local minima and transition structures located on the PESs for the inversion of benzo[c]phenanthrene and the rotation around the Ph–Ph bond in biphenyl catalyzed by coronene (Figure S2); full computational details (Tables S2 and S3); bowl depths of corannulene and sumanene (Table S4); PBE-D3/6-31G(2df,p) optimized geometries (Table S5); B3LYP-D3/Def2-TZVPP optimized geometries (Table S6); and full references for Refs. [34] (GAUSSIAN 09) and [36] (Molpro 2012). Supplementary data associated with this article can be found, in the online version, at doi:[10.1016/j.cplett.2014.09.032](https://doi.org/10.1016/j.cplett.2014.09.032).

#### References

- [1] L.T. Scott, M. Petrukhina, *Fragments of Fullerenes and Carbon Nanotubes: Designed Synthesis, Unusual Reactions, and Coordination Chemistry*, John Wiley & Sons, 2011.
- [2] Y.-T. Wu, J.S. Siegel, *Chem. Rev.* 106 (2006) 4843.
- [3] V.M. Tseffrikas, L.T. Scott, *Chem. Rev.* 106 (2006) 4868.
- [4] B.T. King, *Nat. Chem.* 5 (2013) 730.
- [5] J. Li, et al., *Phys. Chem. Chem. Phys.* 15 (2013) 12694.
- [6] M.R. Kennedy, L.A. Burns, C.D. Sherrill, *J. Phys. Chem. A* 116 (2012) 11920.
- [7] D. Bandera, K.K. Baldridge, A. Linden, R. Dorta, J.S. Siegel, *Angew. Chem. Int. Ed.* 50 (2011) 865.
- [8] A.S. Filatov, M.A. Petrukhina, *Coord. Chem. Rev.* 254 (2010) 2234.
- [9] R. Peverati, K.K. Baldridge, *J. Chem. Theor. Comput.* 4 (2008) 2030.
- [10] H. Sakurai, T. Daiko, T. Hirao, *Science* 301 (2003) 1878.
- [11] T.J. Seiders, K.K. Baldridge, G.H. Grube, J.S. Siegel, *J. Am. Chem. Soc.* 123 (2001) 517.
- [12] L.T. Scott, M.M. Hashemi, M.S. Bratcher, *J. Am. Chem. Soc.* 114 (1992) 1920.
- [13] T. Amaya, H. Sakane, T. Muneishi, T. Hirao, *Chem. Commun.* (2008) 765.
- [14] T. Amaya, T. Hirao, *Chem. Commun.* 47 (2011) 10524.
- [15] M. Juríćek, et al., *Nat. Chem.* 6 (2014) 222.
- [16] A. Karton, B. Chan, K. Raghavachari, L. Radom, *J. Phys. Chem. A* 117 (2013) 1834.
- [17] H. Schneider, *Angew. Chem. Int. Ed.* 48 (2009) 3924.
- [18] V.V. Gobre, A. Tkatchenko, *Nat. Commun.* 4 (2013) 2341.
- [19] P.R. Schreiner, et al., *Nature* 477 (2011) 308.
- [20] S. Grimme, *Chem. Eur. J.* 18 (2012) 9955.
- [21] S. Grimme, *WIREs Comput. Mol. Sci.* 1 (2011) 211.
- [22] L. Goerigk, S. Grimme, *WIREs Comput. Mol. Sci. (Early View)* (2014), <http://dx.doi.org/10.1002/wcms.1193>.
- [23] S. Kozuch, J.M.L. Martin, *Phys. Chem. Chem. Phys.* 13 (2011) 20104.
- [24] S. Kozuch, J.M.L. Martin, *J. Comp. Chem.* 34 (2013) 2327.
- [25] L. Goerigk, S. Grimme, *J. Chem. Theory Comput.* 7 (2011) 291.
- [26] T.H. Dunning Jr., *J. Chem. Phys.* 90 (1989) 1007.
- [27] F. Neese, F. Wenmohs, *ORCA 3.0.1*, Max-Planck-Institute for Bioinorganic Chemistry, Mülheim a. d. Ruhr, Germany, 2012, With contributions from U. Becker, D. Bykov, D. Ganyushin, A.R. Hansen, R. Izsak, D.G. Liakos, C. Kollmar, S. Kossmann, D.A. Pantazis, T. Petrenko, C. Reimann, C. Riplinger, M. Roemelt,

- B. Sandhöfer, I. Schapiro, K. Sivalingam, B. Wezisla, M. Kaláy, S. Grimme and E. Valeev.
- [28] F. Neese, WIREs Comput. Mol. Sci. 2 (2011) 73.
- [29] J.P. Perdew, K. Burke, M. Ernzerhof, Phys. Rev. Lett. 77 (1996) 3865; J.P. Perdew, K. Burke, M. Ernzerhof, Phys. Rev. Lett. 78 (1997) 1396.
- [30] K. Raghavachari, J.S. Binkley, R. Seeger, J.A. Pople, J. Chem. Phys. 72 (1980) 650.
- [31] S. Grimme, J. Antony, S. Ehrlich, H. Krieg, J. Chem. Phys. 132 (2010) 154104.
- [32] A.D. Becke, E.R. Johnson, J. Chem. Phys. 123 (2005) 154101.
- [33] S. Grimme, S. Ehrlich, L. Goerigk, J. Comput. Chem. 32 (2011) 1456.
- [34] M.J. Frisch, et al., Gaussian 09, Revision D.01, Gaussian, Inc., Wallingford, CT, 2009, See also: <http://www.gaussian.com>
- [35] A. Karton, J.M.L. Martin, J. Chem. Phys. 136 (2012) 124114.
- [36] MOLPRO is a package of ab initio programs written by H.-J. Werner, P.J. Knowles, G. Knizia, F.R. Manby, M. Schütz, P. Celani, T. Korona, R. Lindh, A. Mitrushenkov, G. Rauhut, et al. See also: <http://www.molpro.net>
- [37] K.A. Peterson, D. Feller, D.A. Dixon, Theor. Chem. Acc. 131 (2012) 1079.
- [38] A. Karton, S. Daon, J.M.L. Martin, Chem. Phys. Lett. 510 (2011) 165.
- [39] A. Karton, I. Kaminker, J.M.L. Martin, J. Phys. Chem. A 113 (2009) 7610.
- [40] A. Karton, D. Gruzman, J.M.L. Martin, J. Phys. Chem. A 113 (2009) 8434.
- [41] T. Helgaker, W. Klopper, D.P. Tew, Mol. Phys. 106 (2008) 2107.
- [42] J.C. Hanson, C.E. Nordman, Acta Crystallogr. B B32 (1976) 1147.
- [43] R. Jafaar, et al., J. Am. Chem. Soc. (2014) 136, <http://dx.doi.org/10.1021/ja504126z> (in press).
- [44] L. Zoppi, A. Garcia, K.K. Baldridge, J. Phys. Chem. A 114 (2010) 8864.
- [45] A.S. Filatov, E.A. Jackson, L.T. Scott, M.A. Petrukhina, Angew. Chem. Int. Ed. 48 (2009) 8473.
- [46] A.S. Filatov, A.K. Greene, E.A. Jackson, L.T. Scott, M.A. Petrukhina, J. Organomet. Chem. 696 (2011) 2877.
- [47] M. Parschau, et al., Angew. Chem. Int. Ed. 46 (2007) 8258.
- [48] Y. Shen, C.-F. Chen, Chem. Rev. 112 (2012) 1463.
- [49] M.K. Lakshman, et al., J. Am. Chem. Soc. 122 (2000) 12629.